Final published article:
Poulos, A., Miranda, E., & Baker, J. W. (2022). Evaluation of earthquake response spectra directionality using stochastic simulations. *Bulletin of the Seismological Society of America*, 112(1), 307-315.
https://doi.org/10.1785/0120210101

Evaluation of earthquake response spectra directionality using stochastic simulations

Alan Poulos*[1], Eduardo Miranda[1], and Jack W. Baker[1]

[1]Department of Civil and Environmental Engineering, Stanford University, Stanford, California, U.S.A.

Abstract

For earthquake-resistant design purposes, ground motion intensity is usually characterized using response spectra. The amplitude of response spectral ordinates of horizontal components varies significantly with changes in orientation. This change in intensity with orientation is commonly known as ground motion directionality. Although this directionality has been attributed to several factors, such as topographic irregularities, near-fault effects, and local geologic heterogeneities, the mechanism behind this phenomenon is still not well understood. This work studies the directionality characteristics of earthquake ground motion intensity by using synthetic ground motions and comparing their directionality to that of recorded ground motions. The two principal components of horizontal acceleration are sampled independently using a stochastic model based on finite-duration time-modulated filtered Gaussian white-noise processes. By using the same stochastic process to sample both horizontal components of motion, the variance of horizontal ground acceleration has negligible orientation dependence. However, these simulations' response spectral ordinates present directionality levels comparable to those found in real ground motions. It is shown that the directionality of the simulated ground motions changes for each realization of the stochastic process and is a consequence of the duration being finite. Simulated ground motions also present similar directionality trends to recorded earthquake ground motions, such as the increase of average directionality with increasing period of vibration and decrease with increasing significant duration. These results suggest that most of the orientation dependence of horizontal response spectra is primarily explained by the finite significant duration of earthquake ground motion causing inherent randomness in response spectra, rather than by some physical mechanism causing polarization of shaking.

*Corresponding author: apoulos@stanford.edu

INTRODUCTION

Earthquake ground motions are recorded in three orthogonal translational components, one vertical and two in the horizontal plane. The intensity of horizontal components of ground motion, which is usually characterized using response spectra for earthquake-resistant design purposes, varies significantly with changes in orientation. This phenomenon is commonly known as ground motion directionality or polarization. In most cases, the dependence on orientation is disregarded by using a single intensity measure, such as when developing ground motion prediction models or in conventional earthquake-resistant design. One alternative that has been used extensively to define a single intensity measure is to combine the responses in the two as-recorded horizontal orientations by, for example, using their geometric mean or one component at random. Since these methods depend on the orientation of the recording device, some orientation-independent measures have been proposed based on the spectral response over all orientations (Boore et al., 2006; Boore, 2010). Two of the most used measures are the median and the maximum spectral responses from all non-redundant horizontal orientations, which are known as RotD50 and RotD100, respectively (Boore, 2010).

One way to characterize the level of directionality of a spectral response is using the ratio of RotD100 to RotD50, where values close to 1 indicating a low polarization. This ratio is of particular importance for earthquake-resistant design since most of the recent ground motion models have been developed for RotD50 (e.g., Boore et al., 2014) whereas some building codes use RotD100 to define design spectra (e.g., American Society of Civil Engineers, 2016). Thus, some empirical models have been developed for this ratio using recorded ground motions (e.g., Shahi and Baker, 2014; Boore and Kishida, 2017). Other methods that have been used to study directionality are based directly on the ground motion without considering spectral responses, such as those based on polarization analysis (e.g., Vidale, 1986) and on the Arias intensity tensor (e.g., Arias, 1970, 1996).

Several reasons have been given in the literature for the observed ground motion directionality, such as topographic irregularities (e.g, Spudich et al., 1996; Bouchon and Barker, 1996), local geologic heterogeneities (e.g., Bonamassa and Vidale, 1991), basin edge effects (e.g., Heresi et al., 2020), and near-fault effects (e.g., Somerville et al., 1997; Ghayamghamian, 2007). However, all ground motion records present some level of directionality, even when none of the preceding phenomena are present, which suggests that this phenomenon is inherent to any ground motion. For example, spectral amplitudes in the strongest direction are, on average, between 33% and 100% larger (depending on the period of vibration) than those in the perpendicular direction even for recording stations that are far from the earthquake rupture. Furthermore, for a given ground motion, the orientation of the maximum spectral amplitude typically varies significantly with period (Shahi and Baker, 2014), indicating that there is no single 'strongest direction' of a ground motion, as measured using this metric.

This work examines the directionality of ground motions by simulating synthetic accelerograms. The simulation method used is based on filtering and time modulating a Gaussian white noise with finite duration, which accounts for temporal and spectral nonstationarity characteristics of ground motions (Rezaeian and Der Kiureghian, 2008). Both horizontal components of motion are realizations of the same sampling method, and hence the input ground motion is a stochastic process with the same variance over all horizontal orientations. The directionality characteristics of synthetic ground motions are compared to those of real ground motions from shallow crustal

earthquakes in active tectonic regions using the RotD100 to RotD50 ratio. The results are also used to highlight the effect of significant duration on directionality for both the synthetic and real ground motions. Finally, the variance of the synthetic ground motions is modified to reproduce the orientation-dependent variance of real ground motion with the objective of reproducing more realistic directionality characteristics.

GROUND MOTION DIRECTIONALITY

Bidirectional horizontal ground motion records generate spectral ordinates whose amplitudes depend on orientation. As an example, Figure 1a shows the relative displacement trace of a linear elastic single-degree-of-freedom (SDOF) system, with a natural period of vibration of 1.0 seconds and a damping ratio of 5%, when subjected to both horizontal components of the 1989 M_w 6.9 Loma Prieta earthquake recorded in the UCSC Lick Observatory Station, which corresponds to record sequence number 810 in the NGA-West2 database (Ancheta et al., 2014). The as-recorded horizontal components of motion correspond to the horizontal and vertical directions axes of Figure 1a (i.e., 0° and 90°). The figure also shows the spectral acceleration curve for all rotation angles in a polar representation, where the value of spectral acceleration for a given rotation angle is equal to the distance from the curve to the origin. Since, by definition, spectral accelerations are computed using an absolute value, this curve repeats every 180°. The maximum response of the SDOF system for the example ground motion occurs at a rotation angle of approximately $\theta^* = 10^\circ$ with respect to the first horizontal component (0°). This orientation is defined as the major response axis and its perpendicular orientation is the minor response axis (Hong and Goda, 2007). The maximum spectral acceleration (i.e., RotD100) occurs on the major response axis. The spectral acceleration, normalized by RotD100, is shown in Figure 1b as a function of the rotation angle θ to the major response axis, which, following the notation of Hong and Goda (2007), is denoted by

$$\eta(\theta) = \frac{Sa(\theta)}{\text{RotD100}} \tag{1}$$

where $Sa(\theta)$ is the spectral acceleration at a rotation angle θ to the major response axis. Note that there are two lines for the ground motion on Figure 1b, corresponding to clockwise and counterclockwise angles away from the major response axis. The value of $\eta(\theta)$ is always greater than $\cos(\theta)$, which corresponds to a fully polarized response. The response of the SDOF system to this record is quite polarized, with the peak response on the minor axis being only approximately 28% of the peak response on the major axis, i.e. $\eta(90^\circ) = 0.28$.

This study uses two metrics to characterize the directionality of ground motions. The first is $\eta(90^\circ)$ whose value will always be in the $[0, 1]$ range, where zero corresponds to a fully polarized ground motion. Note that for individual records, the minimum value of η may occur at an angle smaller than 90° (e.g., Figure 1b); however, when averaging over several records, the minimum does occur at 90°. The second directionality metric is the ratio between the response in the major axis and the median response (i.e., RotD100/RotD50). The reciprocal of this ratio is represented by the horizontal line shown in Figure 1b. The RotD100 to RotD50 ratio is, by definition, always greater than or equal to 1 and has a maximum value of $\sqrt{2}$, which occurs for a fully polarized ground motion (i.e., one where the response only occurs in a given azimuth), but in many cases fairly polarized responses, such as the one shown in Figure 1, may also have this maximum value.

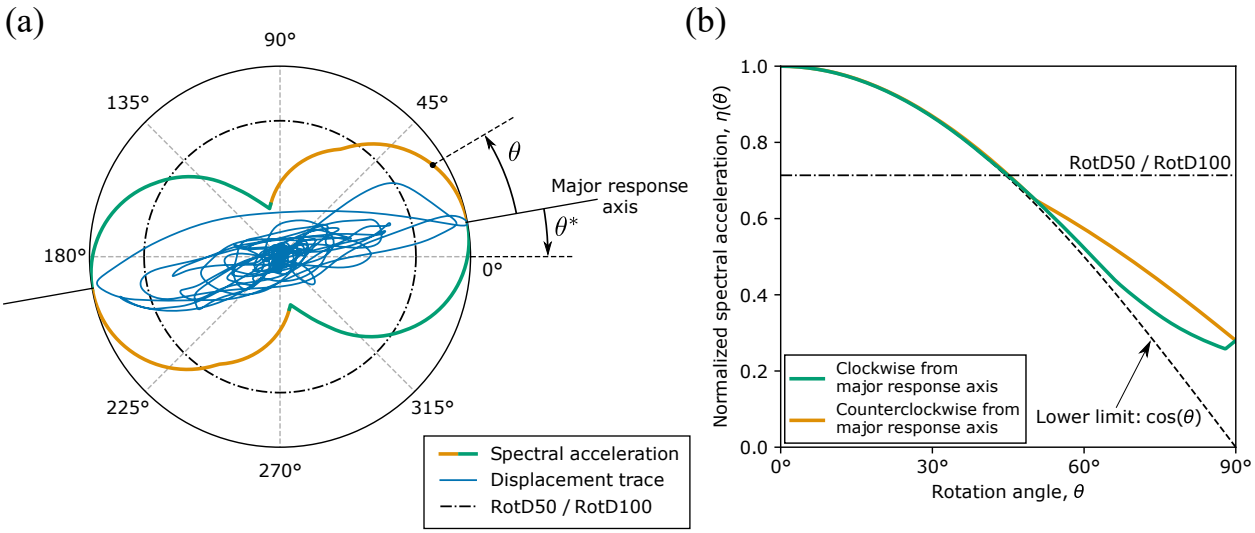

Figure 1: Orientation dependence of the response of a 5%-damped 1.0 s SDOF system when subjected to the horizontal components of record 810 of the NGA-West2 database: (a) relative displacement trace and (b) normalized spectral acceleration as a function of the rotation angle with respect to the major response axis.

GROUND MOTION DATABASE

The directionality of real ground motions was studied using the NGA-West2 database, which contains records from shallow crustal earthquakes in active tectonic regions (Ancheta et al., 2014). In this study, only records with the following characteristics were used: (i) triggered by earthquakes of magnitude greater or equal to 5.0; (ii) recorded in stations with NEHRP site classes B, C, and D; and (iii) recorded in reasonably free-field conditions following the criteria used by Boore et al. (2014). A total of 5,065 pairs of horizontal ground motion records met these criteria, and were applied to 5%-damped SDOF systems with natural vibration periods ranging from 0.01 to 10 s. Each record was only used up to its maximum usable period, which corresponds to the inverse of the lowest usable frequency of each record in the NGA-West2 database.

The mean values of $\eta(\theta)$ from the records of the database are shown in Figure 2 for vibration periods of 0.1, 1, and 10 s. All vibration periods have very similar mean $\eta(\theta)$ values for rotation angles smaller than roughly $\theta = 30°$. However, as one rotates further from the direction where RotD100 occurs, the mean $\eta(\theta)$ varies significantly with period, where on average lower values occur for long periods and higher values for short periods. For example, on average, the spectral acceleration on the minor response axis is 74% of RotD100 for a period of 0.1 s, whereas for a period of 10 s it is only 50% of RotD100. Since the shape of the $\eta(\theta)$ ratio is similar for different periods of vibration, this work focuses on its value on the minor response axis, i.e. $\eta(90°)$.

Figure 3 shows the geometric mean, and several percentiles values of the two directionality metrics, i.e. $\eta(90°)$ and the RotD100 to RotD50 ratio, as a function of period of vibration. Although the values of both metrics exhibit significant between the record-to-record variability in the database, there is a clear trend with changes in the period of vibration. As the period increases, the geometric mean value of $\eta(90°)$ decreases, and the RotD100 to RotD50 ratio increases, which means that, on average, oscillators with longer periods have a more polarized response than those

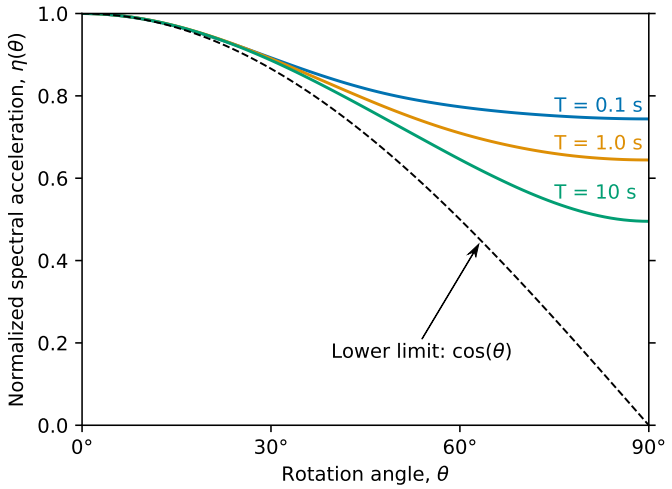

Figure 2: Mean $\eta(\theta)$ of 5,065 pairs of horizontal ground motions from the NGA-West2 database for three periods of vibration.

with shorter periods. Figure 3b also presents the geometric mean of the RotD100 to RotD50 ratio obtained by Shahi and Baker (2014) and Boore and Kishida (2017), which are very similar to the ones obtained in this study, even though they were computed using different subsets of the NGA-West2 database.

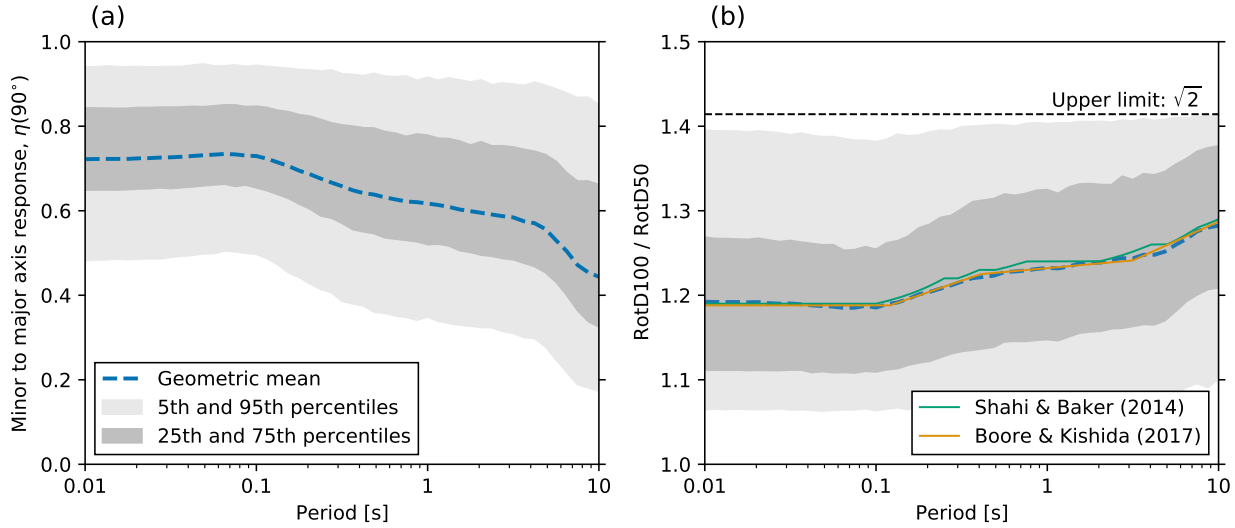

Figure 3: Directionality of ground motions from the NGA-West2 database as a function of period: (a) ratio of minor axis response to major axis response and (b) RotD100 to RotD50 ratio.

SIMULATION OF SYNTHETIC GROUND MOTIONS

Earthquake ground motion simulation methods can be based on physical principles, empirically-calibrated stochastic simulations, or a combination of both (Atkinson and Somerville, 1994; Dou-

glas and Aochi, 2008). Several of the empirical simulation methods are based on a filtered white noise process with finite duration that is modulated in time to account for temporal nonstationarity. A review of the early works based on these time-modulated filtered white noise processes was given by Shinozuka and Deodatis (1988), who suggested that the first work proposing them was presented by Bolotin (1960). This work uses a simulation method based on filtered white noise that was proposed by Rezaeian and Der Kiureghian (2008), which accounts for temporal nonstationarities by using a time modulation function and for spectral nonstationarities by using a linear filter with time-varying parameters. The method starts by sampling a Gaussian white noise (GWN) that is then passed through a linear filter. The resulting signal is then time modulated using a deterministic non-negative time modulation function to account for temporal nonstationarity. Finally, a high-pass filter is applied to the signal to assure that no residual velocity and displacement occurs. Response spectra of ground motions simulated with this method have been found to be similar to the response spectra of recorded ground motions and to have levels of variability that are similar to those of ground motion prediction models (Rezaeian and Der Kiureghian, 2010).

For the simulations in this work, the GWN was generated as independent samples from a standard normal distribution with a sampling frequency of 200 Hz, which is the same frequency typically used in modern accelerographs. The parameters of the linear filter were set to the mean values of the empirical distributions fitted by Rezaeian and Der Kiureghian (2010), and thus do not correspond to any specific earthquake scenario. Note that these distributions were fitted using a ground motion database of 103 horizontal ground motion pairs, which is different to the database used in this study to characterize the directionality of recorded ground motions. However, the directionality characteristics of both databases are very similar. Thus, for comparison purposes, this study uses the larger database to obtain better statistical results. Moreover, the selected time-modulation function had the shape of a gamma distribution, as proposed by Saragoni and Hart (1973). The parameters of the time-modulation function were selected to match a given D_{5-75} significant duration, which is the interval between the times at which 5% and 75% of the Arias intensity is reached (Arias, 1970). The D_{5-75} duration was initially set to the median value from the ground motions database used in this study, which is 12.6 s, although durations corresponding to other percentiles of the distribution were also used for comparison purposes. The simulations were also carried out using time-modulation functions that match a given D_{5-95} significant duration, but only D_{5-75} is presented here because the results of both options are very similar if the same percentile of the respective empirical distributions are used for the simulations. Moreover, other time modulation functions set to have the same significant duration were also used in this study, such as the piecewise function proposed by Jennings et al. (1969), and their results were almost identical to those obtained with the gamma distribution shape.

To show that the results are somewhat independent of the ground motion simulation method, two additional simple methods were also used, which consisted of using the GWN sample directly with and without modulation in time. In this work, these two methods are named time-modulated GWN and GWN, respectively, whereas the method by Rezaeian and Der Kiureghian (2008) is named time-modulated filtered GWN. For the case without time modulation, the duration of the GWN was reduced to be the same as the selected D_{5-75} duration to compensate for the modulation being constant over time. Figure 4 shows example realizations of the three ground motion simulation methods used in this study.

The only source of uncertainty in the three described simulation methods is the initial GWN sample. Independent GWN samples were used for the two horizontal components of ground accel-

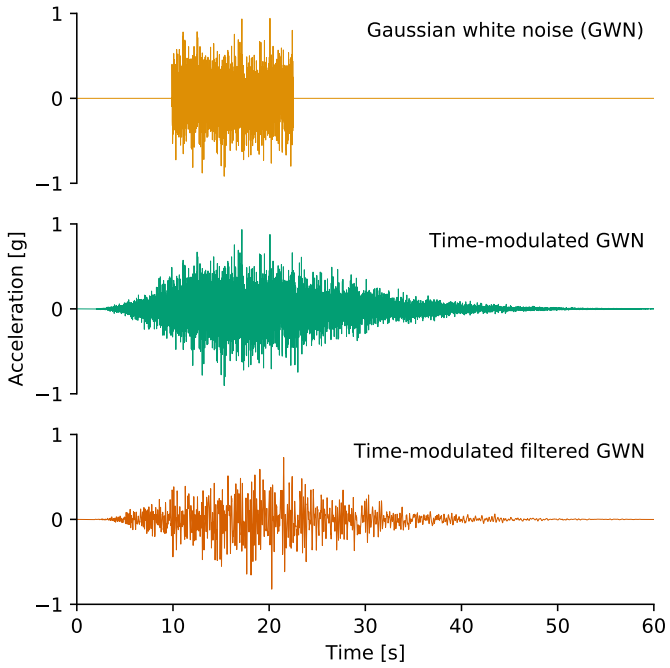

Figure 4: Example realizations of the three ground motion simulation methods using a D_{5-75} duration of 12.6 s.

eration. In general, ground accelerations of two orthogonal horizontal components are correlated, and hence this correlation should be accounted for when sampling the GWN pair. However, if the simulated pair is assumed to be oriented in the principal components of motion (Arias, 1970), this correlation is, by definition, zero. In this work, principal components within the horizontal plane are computed using the entire length of the two horizontal accelerograms. A detailed description of this computation is provided by Rezaeian and Der Kiureghian (2012). Moreover, since the same method is used to sample the acceleration of both horizontal components, the variance of the process is constant over all rotation angles. It is important to note that the value of this variance is irrelevant in this study because the SDOF systems are linear elastic and the directionality metrics are only influenced by relative changes in the response for different rotation angles. Thus, multiplying both horizontal components by the same constant would not change the values of $\eta(90°)$ and the RotD100 to RotD50 ratio.

RESULTS

A total of 2,000 pairs of synthetic ground motions were generated with each of the three simulation methods previously described (i.e., GWN, time-modulated GWN, and time-modulated filtered GWN) and used to compute the bidirectional response of SDOF systems with periods of vibration ranging from 0.01 s to 10 s. The resulting spectral accelerations were then used to compute both directionality metrics. Figure 5a shows the geometric mean $\eta(90°)$ as a function of the period of vibration for the three simulation methods and compares them to the geometric mean values of real ground motions shown from Figure 3a. The three simulation methods resulted in fairly similar

values of $\eta(90^\circ)$ throughout the period range. At short periods, the geometric mean directionality ratios from the simulation methods are greater than those from real ground motions, indicating that real ground motions have, on average, a more polarized response. As the period increases, the differences between the directionality of synthetic and real ground motions become less important, with geometric mean $\eta(90^\circ)$ values being very similar for periods greater than approximately 3 s. Analogous results were obtained for the ratio of RotD100 to RotD50 shown in Figure 5b, where in this case higher ratios indicate more polarization. The geometric mean ratios of the three simulation methods have 99% confidence intervals of approximately ± 0.005, meaning that the finite sample size of the simulations introduces no meaningful uncertainty.

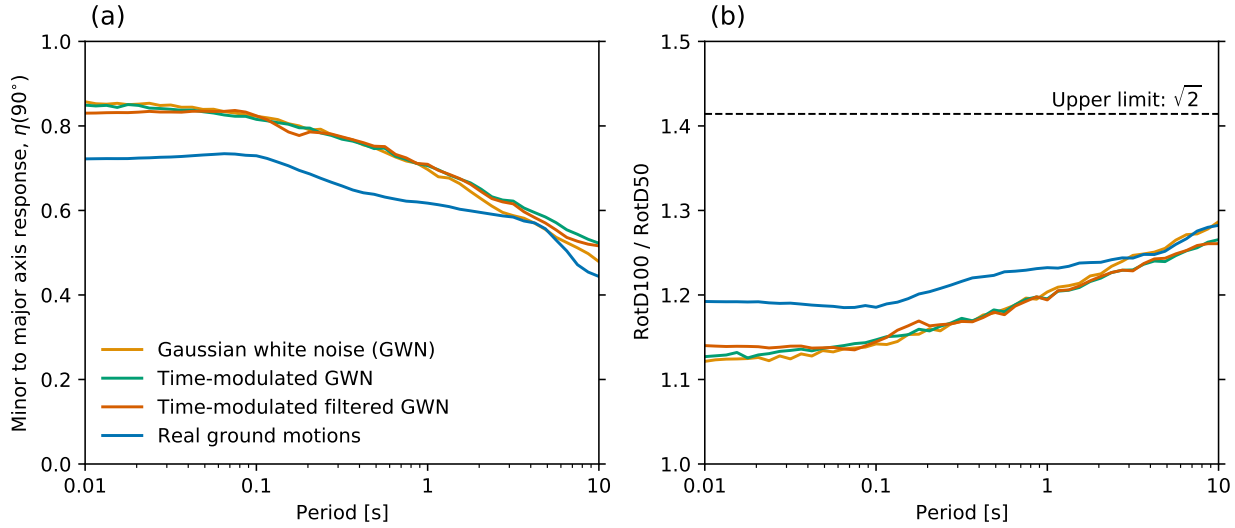

Figure 5: Comparison between the directionality of synthetic ground motions computed with three simulation methods and real ground motions in terms of: (a) geometric mean ratio of minor axis response to major axis response and (b) geometric mean RotD100 to RotD50 ratio. The simulations used a D_{5-75} duration of 12.6 s.

Since both horizontal components of the simulated ground motion have the same variance, their directionality is primarily governed by their duration. To illustrate this observation, the time-modulated GWN method was altered by using the 16$^{\text{th}}$ and 84$^{\text{th}}$ percentiles of the D_{5-75} distribution obtained from the ground motion database, which corresponds to 5.0 and 26.8 s, respectively. The resulting geometric mean RotD100 to RotD50 ratios are presented in Figure 6a, together with the previous result that used the median value of D_{5-75} (Figure 5b). The geometric mean RotD100 to RotD50 ratio decreases (i.e., the motion becomes less polarized) as significant duration increases, regardless of the period of vibration. This is because the SDOF system has more time to oscillate in different directions, resulting in a more homogeneous spectral acceleration as a function of the rotation angle. If D_{5-75} tended to infinity, the RotD100 to RotD50 ratio would be 1. To illustrate this, Figure 6a also shows the geometric mean RotD100 to RotD50 ratios of 2,000 simulations with the significant duration set to D_{5-75} = 1000 s.

The relation between significant duration and directionality occurs not only in synthetic ground motions, it is also present in real ground motions, as shown in Figure 6b, where the ground motion database was grouped in terciles according to D_{5-75}. Analogously to the synthetic ground mo-

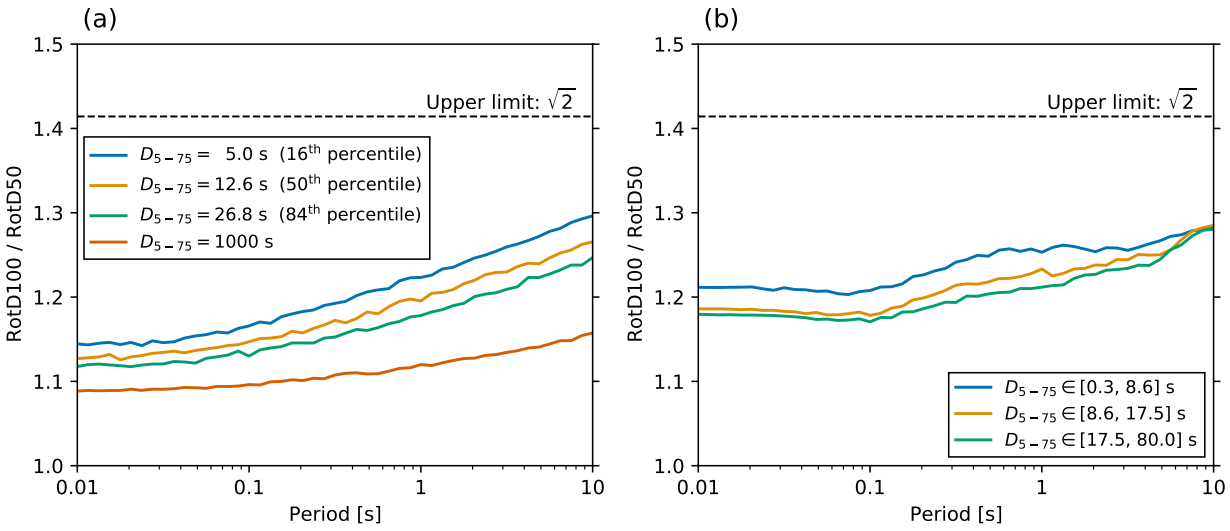

Figure 6: Effect of significant duration on the geometric mean ratio of RotD100 to RotD50 for: (a) synthetic ground motions and (b) real ground motions.

tions, the geometric mean RotD100 to RotD50 ratio of real ground motions also decreases as the significant duration increases, although the trend is less clear for periods longer than approximately 3 s where the number of usable recorded ground motions decreases significantly, which hinders detecting expected differences between the three bins.

To account for the directional dependence of real horizontal ground accelerations in the simulation, the differences in amplitude between both horizontal components were computed using the ground motion database. Each pair of horizontal ground acceleration was first rotated to directions along which both components were uncorrelated (i.e. the principal components of motion) because the simulated ground motion pairs have this orientation. Then, the root mean square, which is equivalent to the standard deviation for zero-mean processes, was computed for both principal components of acceleration within the time interval of D_{5-75} significant duration:

$$\sigma = \sqrt{\frac{1}{t_f - t_i} \int_{t_i}^{t_f} [a(t)]^2 \, dt} \tag{2}$$

where $a(t)$ is the ground acceleration along one of the two principal components of motion in the horizontal plane, and t_i and t_f are the times at which 5% and 75% of the Arias intensity is reached, respectively. Since both horizontal components may have different values of t_i and t_f, the mean times of the two principal components were used in Equation (2). Finally, the maximum of the two standard deviations computed using Equation (2) was divided by the minimum, $\sigma_{\text{max}}/\sigma_{\text{min}}$, resulting in the distribution of ratios shown in Figure 7. The dependence of the computed $\sigma_{\text{max}}/\sigma_{\text{min}}$ ratios on earthquake magnitude and source-to-site distance is small, which is consistent with the results found in previous studies for the RotD100 to RotD50 ratio (Shahi and Baker, 2014; Boore and Kishida, 2017). A gamma distribution was fitted to 1-$\sigma_{\text{max}}/\sigma_{\text{min}}$ using a maximum likelihood estimation, which resulted in a shape parameter of $\alpha = 1.73$ and a rate parameter of $\beta = 6.08$. Note that the fitted distribution is representative of ground motions that satisfy the selection criteria of the database used for calibration (e.g., magnitude ≥ 5).

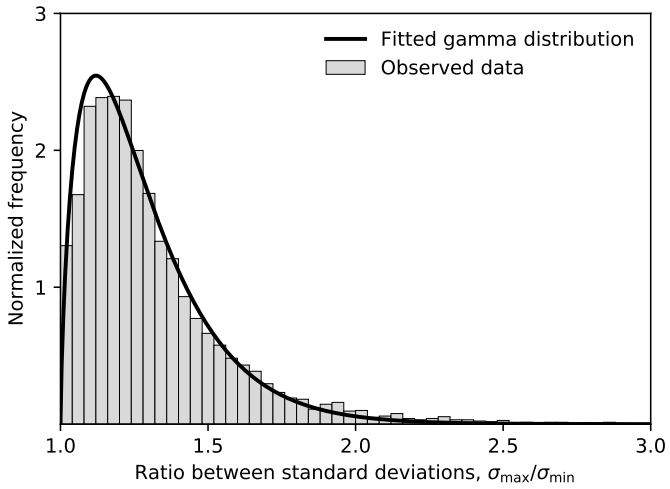

Figure 7: Distribution of the ratio of the maximum standard deviation to the minimum standard deviation between both horizontal components of ground acceleration within the time interval of significant duration.

In order to account for the differences in variances between the two horizontal components, synthetic ground motions simulated using the time-modulated GWN method with D_{5-75} = 12.6 s were modified using the distribution derived from recorded (real) ground motions shown in Figure 7. For each ground motion realization, a standard deviation ratio was sampled from the distribution. Then, one of the simulated horizontal components was scaled by a factor that ensures that the synthetic ground motion had the sampled standard deviation ratio. Although the sampled standard deviation ratio could also be achieved by scaling both horizontal components simultaneously (e.g., such that the average amplitude of both components does not change), the directionality characteristics studied here would be the same because the SDOF systems are linear elastic. Figure 8 shows the geometric mean RotD100 to RotD50 ratio of 2000 realization of this modified simulation method. The results show that once the ratio of standard deviations is set to follow the distribution found from recorded ground motions, then the ratios increase for all periods of vibration, especially for short periods where the differences with real ground motions were higher, reaching values that are very close to those of real ground motions.

CONCLUSIONS

This study has examined the directionality of earthquake ground motions by using synthetic accelerograms. Input ground motions for both horizontal components were simulated by linear filtering and time modulating Gaussian white noise processes with finite duration. The results show that the simulated ground motions, with the same acceleration variance in all directions, have similar directionality characteristics to real ground motions. The similarities are stronger for longer periods of vibration, especially for periods greater than approximately 3 s, where the geometric mean RotD100 / RotD50 of synthetic and real ground motions differ by less than 2%.

It is concluded that the directionality of the synthetic ground motions is primarily a consequence of their duration being finite, since, given an infinite amount of time, the SDOF system

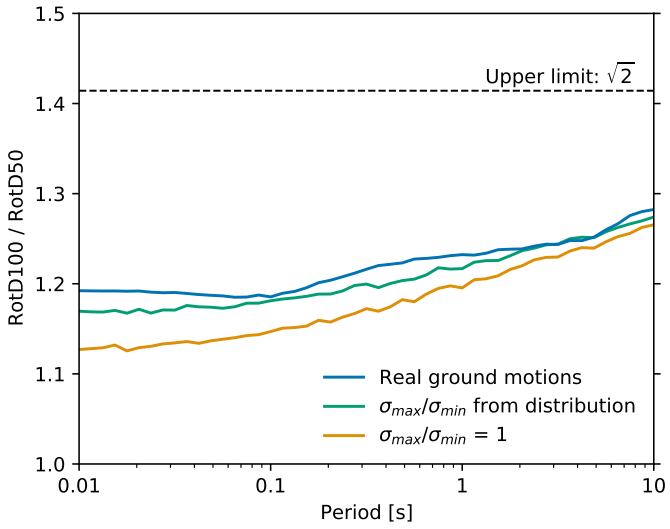

Figure 8: Effect of the ratio of standard deviations between both horizontal components on the geometric mean RotD100 to RotD50 ratio of time-modulated GWN simulations.

will oscillate equally in all orientations. This effect is reflected by the results of the simulations, where the level of directionality decrease with increasing significant duration. A very similar trend was observed using the database of real ground motion records. Another characteristic of ground motion directionality that is well captured by synthetic ground motions is that the average polarization increases with the period of vibration. This is also related to duration because, for the same ground motion, an SDOF system with a long period of vibration will tend to experiment fewer oscillations than those of an SDOF system with a short period. Thus, the longer period SDOF system will tend to have fewer opportunities to respond in different orientations, which will result in a stronger directionality. These effects are related to the peak factor of random vibrations, i.e., the peak response of an oscillator relative to the root-mean-squared response (Cartwright and Longuet-Higgins, 1956), which has been shown to increase with the number of zero crossings (Davenport, 1964; Der Kiureghian, 1980). Both of the variables that were shown to affect directionality (i.e., duration and period of vibration) also affect the peak factor because the number of zero crossings increases with the duration and the mean zero-crossing rate, which is related to the period of vibration.

Adding orientation-dependent variance empirically found from real ground motions to synthetic ground motions results in RotD100 to RotD50 ratios that are even more similar to those of real ground motions. This modification has a larger effect on short period SDOF systems, where the differences in the RotD100 to RotD50 ratios between synthetic and real ground motion are more important, and result in synthetic ground motions that have directionality levels that are very similar to those of real ground motions with similar significant duration over the entire period range.

Real ground motions are much more complex than the idealized synthetic motions used in this work. For example, their changes in amplitude over time are more complex than the gamma distribution function used for the simulations and vary from record to record and even between the two horizontal components of motion. Moreover, significant durations are also orientation-dependent

(Lee, 2014), which was not considered in the simulations. Furthermore, the frequency content of the ground motion and its changes over time might also differ between the two horizontal components (Rezaeian and Der Kiureghian, 2012). However, despite these differences, the idealized synthetic ground motions used in this study still have levels of directionality that are very similar to those of real ground motions, suggesting that most of the directionality of earthquake ground motions can be attributed to the inherent randomness of peak responses to finite-duration loading. This does not mean that other possible causes of highly polarized ground motions, such as rupture effects in the near field, topographic irregularities, and local geologic heterogeneities, should be disregarded, but simply that significant levels of ground motion directionality should be expected even when none of these factors are present.

DATA AND RESOURCES

The ground motion records used in this study were obtained from the NGA-West2 ground motion database developed by the Pacific Earthquake Engineering Research Center (http://ngawest2.berkeley.edu/spectras/new, last accessed April 2020).

ACKNOWLEDGMENTS

The authors would like to acknowledge the National Agency for Research and Development (ANID) / Doctorado Becas Chile / 2019-72200307 and the Nancy Grant Chamberlain Fellowship at Stanford University for sponsoring the doctoral studies of the first author. The authors also thank Rodrigo Silva-Lopez for providing helpful feedback.

REFERENCES

American Society of Civil Engineers (2016). *Minimum design loads and associated criteria for buildings and other structures* (ASCE/SEI 7-16 ed.). American Society of Civil Engineers, Reston, VA.

Ancheta, T. D., R. B. Darragh, J. P. Stewart, E. Seyhan, W. J. Silva, B. S.-J. Chiou, K. E. Wooddell, R. W. Graves, A. R. Kottke, D. M. Boore, et al. (2014). NGA-West2 database, *Earthq. Spectra* **30**, 989–1005.

Arias, A. (1970). A measure of earthquake intensity. In R. J. Hansen (Ed.), *Seismic Design for Nuclear Power Plants*, 438–483. MIT Press, Cambridge, MA.

Arias, A. (1996). Local directivity of strong ground motion. In *Proceedings of the 11th World Conference on Earthquake Engineering*, Acapulco, Mexico.

Atkinson, G. M. and P. G. Somerville (1994). Calibration of time history simulation methods, *Bull. Seismol. Soc. Am.* **84**, 400–414.

Bolotin, V. V. (1960, July). Statistical theory of the aseismic design of structures. In *Proceedings of the 2nd World Conference on Earthquake Engineering*, Volume II, Tokyo and Kyoto, Japan, 1365–1374.

Bonamassa, O. and J. E. Vidale (1991). Directional site resonances observed from aftershocks of the 18 October 1989 Loma Prieta earthquake, *Bull. Seismol. Soc. Am.* **81**, 1945–1957.

Boore, D. M. (2010). Orientation-independent, nongeometric-mean measures of seismic intensity from two horizontal components of motion, *Bull. Seismol. Soc. Am.* **100**, 1830–1835.

Boore, D. M. and T. Kishida (2017). Relations between some horizontal-component ground-motion intensity measures used in practice, *Bull. Seismol. Soc. Am.* **107**, 334–343.

Boore, D. M., J. P. Stewart, E. Seyhan, and G. M. Atkinson (2014). NGA-West2 equations for predicting PGA, PGV, and 5% damped PSA for shallow crustal earthquakes, *Earthq. Spectra* **30**, 1057–1085.

Boore, D. M., J. Watson-Lamprey, and N. A. Abrahamson (2006). Orientation-independent measures of ground motion, *Bull. Seismol. Soc. Am.* **96**, 1502–1511.

Bouchon, M. and J. S. Barker (1996). Seismic response of a hill: the example of Tarzana, California, *Bull. Seismol. Soc. Am.* **86**, 66–72.

Cartwright, D. E. and M. S. Longuet-Higgins (1956). The statistical distribution of the maxima of a random function, *Proc. R. Soc. Lond. A* **237**, 212–232.

Davenport, A. G. (1964). Note on the distribution of the largest value of a random function with application to gust loading, *Proc. Inst. Civ. Eng.* **28**, 187–196.

Der Kiureghian, A. (1980). Structural response to stationary excitation, *J. Eng. Mech. Div. ASCE* **106**, 1195–1213.

Douglas, J. and H. Aochi (2008). A survey of techniques for predicting earthquake ground motions for engineering purposes, *Surv. Geophys.* **29**, 187.

Ghayamghamian, M. R. (2007). Directional damage due to near-fault and site effects in the M6.4 Changureh–Avaj earthquake of 22 June 2002, *J. Seismol.* **11**, 39–57.

Heresi, P., J. Ruiz-García, O. Payán-Serrano, and E. Miranda (2020). Observations of Rayleigh waves in Mexico City Valley during the 19 September 2017 Puebla–Morelos, Mexico earthquake, *Earthq. Spectra* **36**, 62–82.

Hong, H. P. and K. Goda (2007). Orientation-dependent ground-motion measure for seismic-hazard assessment, *Bull. Seismol. Soc. Am.* **97**, 1525–1538.

Jennings, P. C., G. W. Housner, and N. C. Tsai (1969, January). Simulated earthquake motions for design purposes. In *Proceedings of the 4th World Conference on Earthquake Engineering*, Volume A-1, Santiago, Chile, 145–160.

Lee, J. (2014, July). Directionality of strong ground motion durations. In *Proceedings of the 10th US National Conference on Earthquake Engineering*, Anchorage, AK.

Rezaeian, S. and A. Der Kiureghian (2008). A stochastic ground motion model with separable temporal and spectral nonstationarities, *Earthq. Eng. Struct. Dynam.* **37**, 1565–1584.

Rezaeian, S. and A. Der Kiureghian (2010). Simulation of synthetic ground motions for specified earthquake and site characteristics, *Earthq. Eng. Struct. Dynam.* **39**, 1155–1180.

Rezaeian, S. and A. Der Kiureghian (2012). Simulation of orthogonal horizontal ground motion components for specified earthquake and site characteristics, *Earthq. Eng. Struct. Dynam.* **41**, 335–353.

Saragoni, G. R. and G. C. Hart (1973). Simulation of artificial earthquakes, *Earthq. Eng. Struct. Dynam.* **2**, 249–267.

Shahi, S. K. and J. W. Baker (2014). NGA-West2 models for ground motion directionality, *Earthq. Spectra* **30**, 1285–1300.

Shinozuka, M. and G. Deodatis (1988). Stochastic process models for earthquake ground motion, *Prob. Eng. Mech.* **3**, 114–123.

Somerville, P. G., N. F. Smith, R. W. Graves, and N. A. Abrahamson (1997). Modification of empirical strong ground motion attenuation relations to include the amplitude and duration effects of rupture directivity, *Seismol. Res. Lett.* **68**, 199–222.

Spudich, P., M. Hellweg, and W. H. K. Lee (1996). Directional topographic site response at Tarzana observed in aftershocks of the 1994 Northridge, California, earthquake: implications for mainshock motions, *Bull. Seismol. Soc. Am.* **86**, S193–S208.

Vidale, J. E. (1986). Complex polarization analysis of particle motion, *Bull. Seismol. Soc. Am.* **76**, 1393–1405.

Department of Civil and Environmental Engineering
Stanford University
473 Via Ortega
Stanford, California 94305, U.S.A.
apoulos@stanford.edu
emiranda@stanford.edu
bakerjw@stanford.edu